Journal of Thermal Analysis and Calorimetry, Vol. 69 (2002) 465–485

CALORIMETRIC ANALYSIS OF VESICULAR SYSTEMS

S. A. Leharne[*]

Centre for Contaminated Land Remediation and Biocalorimetry Centre, Medway Sciences, Natural Resources Institute, University of Greenwich, Central Avenue, Chatham Maritime, Kent, ME4 4AW, UK

(Received April 16, 2002)

Abstract

A number of studies of micellar aggregation in aqueous solutions of ethylene oxide-propylene oxide block copolymers – using high sensitivity differential scanning calorimetry (HSDSC) – are reviewed. The review attempts to show how the calorimetric output can be analysed, using a model fitting procedure, to obtain estimates for various thermodynamic parameters, which characterise the micellization event, as observed by HSDSC. These important parameters include:

- $T_{1/2}$ the temperature at which half the surfactant has been incorporated into micelles;
- ΔH_{cal} – the calorimetric enthalpy for the process which is measured by integration of the calorimetric output;
- ΔH_{vH} – the van't Hoff enthalpy – which characterises the functional dependence of the equilibrium composition of the system upon temperature and which is derived from the application of the van't Hoff isochore to the data analysis procedure;
- ΔC_p – the heat capacity change between the initial and final states;
- and n the aggregation number.

Using this data it is possible to examine how extent of aggregation functionally varies with temperature. Subsequent interpolation of these thermal aggregation plots permits an examination of how the extent of aggregation is affected by changes in solution composition under isothermal conditions. A large body of data is presented which shows how co-solvents, co-solutes and pH affect the aggregation process in aqueous solution.

Keywords: calorimetry, vesicular systems

Introduction

Ethylene oxide-propylene oxide-ethylene oxide block copolymeric surfactants – commonly called poloxamers, synperonics or pluronics – are widely used as laundry aids, detergents, dispersion stabilisers, emulsifiers, solubilizing agents and controlled

* Author for correspondence: E-mail: s.a.leharne@gre.ac.uk

1418–2874/2002/ $ 5.00
Akadémiai Kiadó, Budapest

release agents in the pharmaceutical industry, as bio-processing aids and as components in ink production [1]. These surfactants are ABA block copolymers which have the following structure:

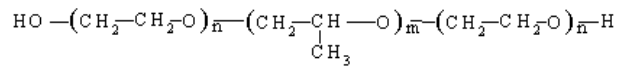

The central block is synthesised from propylene oxide (PO) and provides the molecule with its necessary hydrophobicity. Hydrophilic ethylene oxide (EO) blocks – of equal length – are attached either side of this central moiety. Manipulation of the EO and PO block lengths provides a mechanism whereby the surface activity of the surfactants is readily controlled.

These copolymers show the unusual property of aggregating to form micelles upon warming, a phenomenon which has attracted much research interest. Self-aggregation arises because the central PO block – which in common with the EO blocks is reasonably water-soluble at low temperatures – becomes increasingly hydrophobic as the temperature is raised. Attempts to understand this phenomenon have proceeded by considering the aqueous solubility of EO and PO homopolymers as a function of temperature. It has been proposed [2] that EO chains – in water – may be accommodated within an ice like structure. The formation of such a structure produces a favourable (exothermic) enthalpy change but also results in an entropy penalty associated with the enhanced structuring of water. At low temperatures this enthalpy contribution together with the combinatorial entropy contribution of the chains, to the free energy of mixing, outweighs the entropy penalty. However an increase in temperature reverses this balance, giving rise to phase separation. The theory may also be used to account for the solubility of PO polymers in water. In this case however the pendant methyl group produces a strain in the ice-like structure of water in the hydration sphere which results in phase separation at lower temperatures [2]. Such an explanation though is not without controversy. Finney and Soper [3] using neutron scattering have not found any evidence for such structuring around non-polar methyl groups. Other workers have proposed that the origin of the increasing hydrophobicity in EO homopolymers is the result of changing conformations of EO segments [3]. For the backbone segments –O–C–C–O– the preferred orientation about the bonds is trans-gauche-trans [4, 5]. In such polar conformational states interaction with water is favoured, there being, on average, some two water molecules per EO unit [5]. This state is of low energy but also of low statistical mass, there being only two of these conformations [4]. At higher temperatures less polar orientations are favoured. These are of higher energy but of higher statistical mass – there being some 23 non-polar conformations. Self-evidently the less polar conformations interact less favourably with water. The resulting loss of water at higher temperatures permits EO chains to come together. This model has been used with some success to explain phase separation of EO in aqueous solutions [4] and non-aqueous solvents [6]. The changes in C–C bonds from gauche to trans, thereby altering the polarity, has been confirmed by ^{13}C NMR [6, 7].

Micellization in EO–PO–EO block copolymers is understood to arise for similar reasons. [1, 8]. As the temperature of a block copolymer solution is raised the PO block progressively loses its hydration sphere resulting in a greater interaction between PO blocks on different chains. The EO blocks on the other hand retain their strong interaction with water thus, as is common for all amphiphilic molecules, the differing phase preferences of the blocks drives the copolymers to form micelles.

Micellization in aqueous solutions of these block copolymers has been examined using a wide variety of physical techniques [9]. Of interest to this present study is the observation that the strongly endothermic nature of the micellization process permits an examination of the thermodynamics of the transition using high sensitivity differential scanning calorimetry [10, 11]. It is worth noting that the strong endothermic nature of the micellisation process also signifies that micellisation has a strong temperature dependence. Thus the critical micellisation concentration (cmc) is extremely sensitive to temperature changes. Moreover the cmc of these systems is also heavily dependent upon the molecular composition of the copolymers [11].

DSC instrumentation

The DSC scans provided in the review were all captured using a MicroCal MC2 high sensitivity differential scanning calorimeter (HSDSC) (*ex* MicroCal, Northampton, MA, USA). The cells in this instrument are fixed and are filled and emptied using syringes. Clearly only liquid samples can be investigated. There is a hundred function thermopile between the reference and sample cells which senses the off balance temperature between them and produces a corresponding voltage. The amplified voltage is used to drive the auxiliary heater on the sample cell, which then acts to keep the off-balance temperature between the cells close to zero. A signal proportional to the differential electrical power supplied to both cells can then be recorded (the Y-axis) as a function of temperature (the X-axis). The power data have the units of J s^{-1} this can be converted to the apparent excess heat capacity ($C_{p,xs}$; J mol^{-1} K^{-1}) by normalising the power data with respect to scan rate (σ; K s^{-1}) and number of moles of material placed in the calorimeter (M; mol).

$$C_{p,xs} = \frac{\text{power}}{\sigma M}$$

DSC data analysis

Figure 1 provides an example of the output obtained – using the MC2 – for thermally induced micellization in an aqueous solution of the syperonic P217 (molecular formula: $EO_{52}PO_{34}EO_{52}$; solution concentration 5 mg mL^{-1}; scan rate 60 K h^{-1}). An important first step in the analysis of these systems is the demonstration that the signal is obtained under thermodynamic equilibrium conditions. This can be achieved experimentally by confirming that the signal is independent of scan rate [12]. An example of scan-rate independence is shown in Fig. 2. In the diagram thermal data obtained

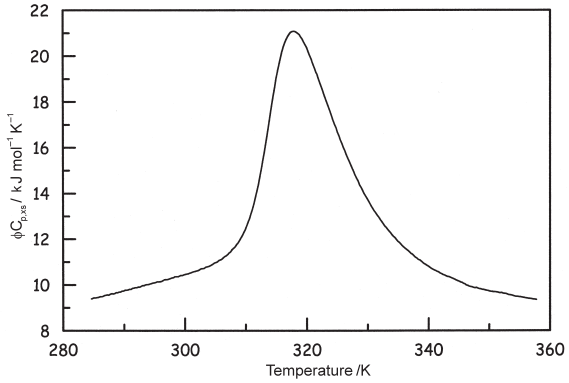

Fig. 1 Apparent excess heat capacity, $\phi C_{p,xs}$, as a function of temperature, for the micellization transition in a 20 g dm^{-3} aqueous solution of P217. Molecular formula of P217 is $EO_{52}PO_{34}EO_{52}$

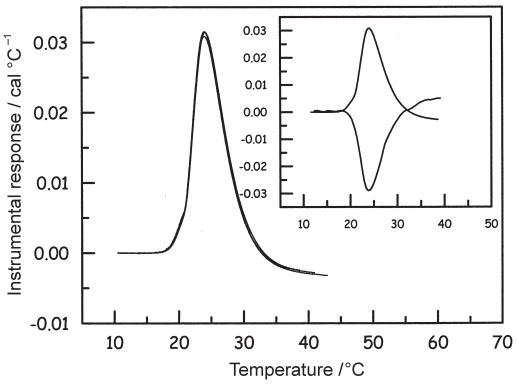

Fig. 2 HSDSC data obtained for P333 ($EO_{17}PO_{60}EO_{17}$) at a variety of scan-rates (10–60 K h^{-1}) to show the scan rate independence of the HSDSC output. The inset shows the HSDSC output obtained in the up-scan and down-scan mode, both at a scan rate of 30 K h^{-1}

for P333 ($EO_{17}PO_{60}EO_{17}$) solutions (of 10 g dm^{-3} concentration) at scan rates of 10, 30 and 60 K h^{-1} can be superimposed on each other. Moreover the diagram further illustrates that the up-scan, obtained at a scan rate of 30 K h^{-1}, is the mirror image of the down-scan at the same scan rate. Both sets of evidence confirm the applicability of thermodynamics to the analysis of the DSC data. If the processes represented by the signals are under thermodynamic control then it should be possible to use the van't Hoff relationship which functionally relates changing composition in the aqueous system of interest to changes in temperature to characterise these signals. This is the aim of the data analysis procedures outline below.

The shape of the signal shown in Fig. 1 is indicative of aggregation [13]. And it can be shown that the onset of aggregation corresponds to the formation of micelles as detected by light scattering and the emergence of micellar properties such as

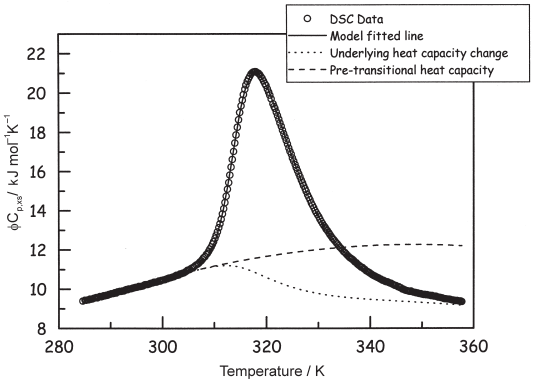

Fig. 3 Model fitting result using the data shown in Fig. 1

solubilisation [1]. Clearly data analysis requires a suitable model of aggregation on which to flesh out a comprehensive procedure to analyse the data.

In DSC the observed change in enthalpy with respect to temperature for a process under strict thermodynamic control is given by [13]:

$$\frac{\mathrm{d}q_\mathrm{p}}{\mathrm{d}T}=\phi C_{\mathrm{p,xs}}=\frac{\mathrm{d}}{\mathrm{d}T}\alpha[\Delta H_{\mathrm{cal}}(T_{1/2})+\Delta C_\mathrm{p}(T-T_{1/2})] \tag{1}$$

where q_p is the heat change at constant pressure; T is temperature; $\phi C_{\mathrm{p,xs}}$ is the apparent excess heat capacity (i.e. the difference in heat capacity between the reference and sample cells); α is the extent of change in the system; $\Delta H_{\mathrm{cal}}(T_{½})$ is the experimentally determined enthalpy change at $T_{½}$ the temperature at which α equals 0.5 and ΔC_p is the difference in heat capacity between the initial and final states of the system.

Given the temperature independence of $T_{½}$ and $\Delta H_{\mathrm{cal}}(T_{½})$ and assuming ΔC_p is independent of temperature for the system of interest, the above equation may be rewritten as:

$$\phi C_{\mathrm{p,xs}}=\frac{\mathrm{d}\alpha}{\mathrm{d}T}[\Delta H_{\mathrm{cal}}(T_{1/2})+\Delta C_\mathrm{p}(T-T_{1/2})]+\alpha\Delta C_\mathrm{p} \tag{2}$$

The extent of conversion to micelles, α, for the aqueous surfactant systems examined in this work is obtained from the temperature dependence of the equilibrium constant describing the incorporation of surfactant unimers into micelles:

$$\left(\frac{\partial \ln K(T_{1/2})}{\partial T}\right)_\mathrm{p}=\frac{\Delta H_{\mathrm{vH}}+\Delta C_\mathrm{p}\dfrac{\Delta H_{\mathrm{vH}}}{\Delta H_{\mathrm{cal}}}(T-T_{1/2})}{RT^2} \tag{3}$$

where ΔH_{vH} is the van't Hoff enthalpy.

A few brief comments about the van't Hoff enthalpy are appropriate. The van't Hoff enthalpy is the enthalpy value that controls the temperature dependence of the equilibrium constant. In the vesicular systems under consideration in this review

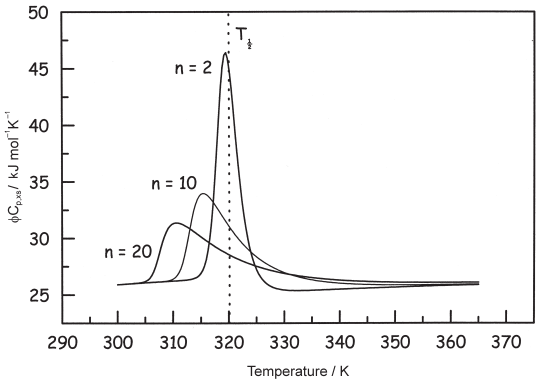

Fig. 4 Impact of aggregation number upon the shape and size of the thermal aggregation signal. The following parametric values were used: ΔH_{cal}=100 kJ mol^{-1}, ΔH_{vH}=1000 kJ mol^{-1}, $T_{1/2}$=320 K and ΔC_p= –15 kJ mol^{-1} K^{-1}

the van't Hoff enthalpy therefore describes how the composition of the solution – in terms of unimer and micelle concentrations – alters with temperature. This information is actually contained within the shape and dimensions of the DSC curve as shown in Fig. 6. It is interesting to note that molar unit in the van't Hoff enthalpy is supplied by the universal gas constant, *R*. Thus the molar unit in the van't Hoff enthalpy describes the basic unit of the system that is involved in the process. The user, on the other hand, supplies the molar unit in the calorimetric enthalpy. That is the user concentration normalises the heat capacity data by dividing the power data by the number of moles of chains placed in the DSC cell. The ratio of the van't Hoff enthalpy and the calorimetric enthalpy therefore provides a measure of the size of the co-operative unit involved in the micellization process. In other words it reports on the number of molecules that co-operate with each other to effect the change seen in the calorimeter. The heat capacity change in Eq. (3) is therefore scaled to reflect this co-operatively in the system since the equilibrium constant reflects those processes involving this co-operative unit. $K(T)$ can be obtained by integrating Eq. (3) and this value can be used in the following mass action Eq. (14) to evaluate the fraction of surfactant in micellar form:

$$K(T)=\frac{[X_n]}{[X]^n}=\frac{\frac{\alpha C}{n}}{((1-\alpha)C)^n} \tag{4}$$

where X is the copolymer in unimeric form (this term actually denotes the co-operative units that combine together to form the micellar aggregates); X_n is the copolymer micelle; n is the aggregation number and C is the initial concentration of copolymer. The evaluation of α at various temperatures permits an evaluation of the temperature dependence of $\phi C_{p,xs}$ in Eq. (2).

Using this series of equations provides a mechanism for model fitting the DSC signals and for obtaining the values for the various thermodynamic parameters appearing in the above equations. The general form for a dissociation transition is simply the reciprocal of Eq. 4.

In our earlier publications data fitting was accomplished by identifying the pre-transitional portion of the base line, which was then fitted to a linear regression line. This line was then subsequently subtracted from the entire data set thereby essentially setting the pre-transitional portion of the apparent excess heat capacity to zero. In more recent data analyses the pre-transitional portion is fitted to a quadratic line. This is undertaken at the same time as the substantive signal is fitted to the thermodynamic model outlined above.

The result of model fitting the DSC output presented in Fig. 1 is shown in Fig. 3. There is clearly a very good match between the obtained data and the model fitting exercise. Table 1 provides some indication of the values obtained for the various fitted parameters obtained for a 5 g dm^{-3} solution of P237 ($EO_{61}PO_{40}EO_{61}$).

Table 1 Fitted parameter values obtained for a 5 g dm^{-3} solution of P237 ($EO_{61}PO_{40}EO_{61}$)

H_{cal} (kJ mol^{-1})	268
H_{vH} (kJ mol^{-1})	848
$T_{1/2}$ (K)	319.6
n	8.8
C_p (kJ mol^{-1} K^{-1})	–11.3

The excellent correspondence between the model and experimental data affords confidence in the molecular description of the micellar aggregation event. It is worth noting that calorimetry does not provide molecular details of the processes which give rise to the thermal signals. However, the simple mass action description of aggregation clearly supplies a useful description, at the molecular level, of micelle formation. In this sense the model fitting process is extremely useful because it aids interpretation of the thermal events as reported by the calorimeter.

The model as outlined and applied pre-supposes that the aggregates are of an invariant size. This is not the case. In these systems the numbers of molecules incorporated into micellar aggregates is known to increase with temperature [1]. This conflict between a constant aggregation number in the model and an experimentally observed increase in aggregation number with temperature is readily resolved. It has been argued [38] that the aggregation process observed by the HSDSC is in effect a nucleation event and provides the endothermic signal which originates from the destruction of the hydrogen bonded structure of the water of hydration associated with the PO blocks. Growth is calorimetrically silent and probably occurs by way of exchange of molecules between micelles. Since they are already dehydrated there is no enthalpic signal associated with the exchange. Micellar growth may however contribute to changes in the post-transitional heat capacity [38].

It is striking that the values obtained for ΔH_{vH} and ΔH_{cal} are different and – as alluded to previously – reflect the difference in the way they were evaluated. More precisely they reflect a difference in what is perceived to be the molar unit in the enthalpic dimensions. ΔH_{cal} is obtained directly by integration of the HSDSC trace and the mole referred to in its units is based upon the mass of copolymer chains placed in the cell. The number of moles of chains is given by the ratio of mass/molar mass of P237. It can be shown, using the above equations, that ΔH_{vH} is given by the following equation:

$$\Delta H_{vH} = \frac{2(n+1)C_{p,1/2}RT_{1/2}}{\Delta H_{cal}} \quad (5)$$

where $C_{p,1/2}$ is the apparent excess heat capacity at $T_{1/2}$ and the other symbols have their previously defined meanings. Equation (5) clearly demonstrates that since both $C_{p,1/2}$ and ΔH_{cal} have the same molar definition which cancels out the molar definition for ΔH_{vH} is correspondingly supplied by the gas constant, R, which is the proportionality constant obtained from the van't Hoff isochore. The fact that the ratio $\Delta H_{vH}/\Delta H_{cal}$ is greater than 1 for all the solutions studied indicates that the molar reaction unit involved in the aggregation process is composed of several chains. This is the unit involved in the reaction and described in the equilibrium equations as X. The van't Hoff enthalpy/calorimetric enthalpy ratio our work suggests that some 3 molecules comprise these pre-micellar aggregates. Interestingly Hergeth *et al.* [5] suggest that at low poloxamer concentrations and thus at temperatures below which we would observe aggregation by HSDSC [10, 11], these block copolymers are encountered predominantly as unimers, dimers and trimers. Hecht and Hoffmann using T Jump experiments and light scattering to determine micellar characteristics also concluded that pre-micellar aggregates are formed prior to micelle formation [37].

How do the values of the characteristic parameters affect the signal?

The ability of the outlined model to capture the major features of the aggregation process in aqueous solutions of the EO–PO–EO block copolymers provides us with a tool whereby we can model how the signal may change as the parameters characterising the aggregation process change.

Figure 4 displays model simulated output which was obtained from an investigation of the impact of increasing aggregation number (n) upon the calorimetric signal. Recall n is the number of reaction units that aggregate together to form micelles. Our analysis suggests that this process involves aggregation of trimeric aggregates. The most notable features associated with the change are the increasing asymmetry of the signals and the fact that the onset of the aggregation process is lowered as n increases. One feature of the model output is the seeming paradox that as n increases the area under the curve on the low temperature side of $T_{1/2}$ becomes increasingly greater than the area under the curve on the high temperature side. This seeming paradox is

readily resolved by plotting a thermal speciation diagram. Such a diagram shows how the fraction of species alters as a function of temperature. Such a diagram is readily constructed by integrating Eq. (3) between the limits of T – the temperature of interest and $T_{1/2}$.

$$K(T)=K(T_{1/2})\exp\left\{\frac{\Delta H_{vH}}{R}\left[\frac{1}{T_{1/2}}-\frac{1}{T}\right]+\frac{\Delta C_p}{R}\left[\ln\left(\frac{T}{T_{1/2}}\right)+\frac{T_{1/2}}{T}-1\right]\right\} \quad (6)$$

Recalling that α=0.5 at $T_{1/2}$ the product of $K(T)/K(T_{½})$ can be written – using Eq. (4) – as:

$$\frac{K(T)}{K(T_{1/2})}=\frac{\alpha\, 0.5^{n-1}}{(1-\alpha)^n} \quad (7)$$

Equation (7) can be solved for various temperatures and the resultant values for can then plotted *vs*. *T*.

In Fig. 5 the fraction of aggregated material is shown as a function of temperature using the model data that was used to create Fig. 4. The plot confirms that at $T_{1/2}$ the fraction of material in the aggregated form is indeed 0.5. However in line with the sharpness of the transition for n=2, the fraction aggregated rapidly reaches 1 on the high temperature side. On the other hand for the case where the aggregation number is 30 it is clear that less than 100% of material is incorporated in micellar aggregates even at high temperatures. The rest of the material is presumably remains in solution in its pre-micellar form.

It is also important to appreciate that the failure of a sizeable fraction of the copolymer to be incorporated into micellar aggregates for the cases of n=10 and n=30 means that the integrated area of the thermal signals is likely to be less than the true value for the calorimetric enthalpy. Integration of the peaks shown in Fig. 4 reveals that the measured calorimetric enthalpies are 96 (for n=2), 86 (for n=10) and 58 (for

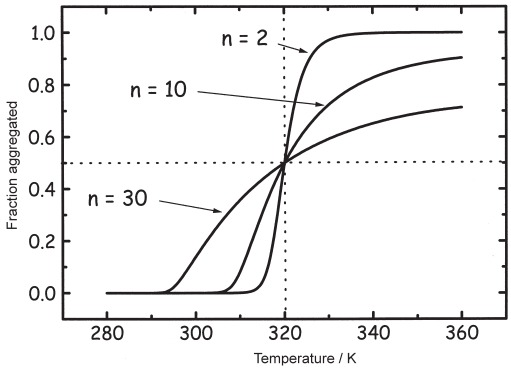

Fig. 5 Thermal speciation graph showing how the fraction of aggregated copolymer varies functionally with temperature for different aggregation numbers. The parametric values used in Fig. 4 were used to generate the curves

n=30) kJ mol^{-1} respectively. Clearly care is necessary when interpreting these signals. Interestingly however use of the outlined model – in which the calorimetric enthalpy is a fitted parameter – does return the correct value for the calorimetric enthalpy.

The impact of changing the van't Hoff enthalpy and concomitant scaled change in the heat capacity has been modelled and the output is shown in Fig. 6. As the van't Hoff enthalpy decreases the transition becomes broader. And as Fig. 7 demonstrates the fraction of copolymer that is ultimately encountered in aggregated form

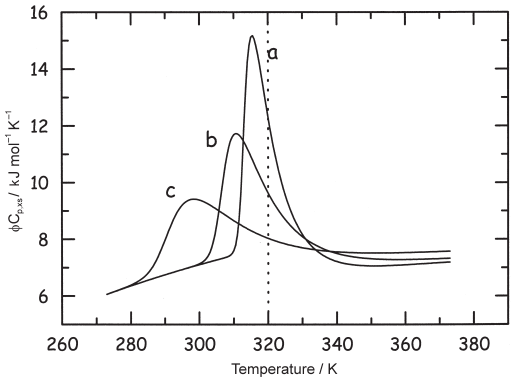

Fig. 6 Impact of van't Hoff enthalpy and heat capacity changes upon the aggregation transition. All the transitions have the same following parametric values: ΔH_{cal}=100 kJ mol^{-1}; $T_{1/2}$=320 K; n=10, van't Hoff enthalpy and heat capacity data are as follows: a – ΔH_{vH}=1000 kJ mol^{-1}; ΔC_p= –15 kJ mol^{-1} K^{-1}; b – ΔH_{vH}=500 kJ mol^{-1}; ΔC_p= –7.5 kJ mol^{-1} K^{-1} and c – ΔH_{vH}=200 kJ mol^{-1}; ΔC_p= –3 kJ mol^{-1} K^{-1}

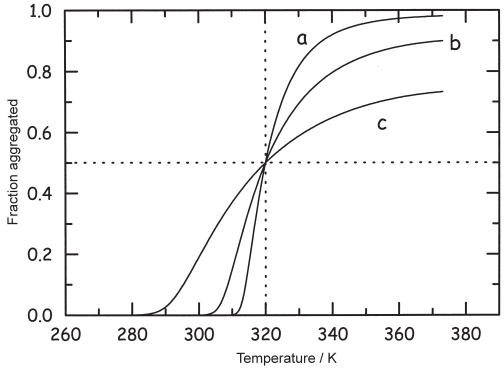

Fig. 7 Impact of van't Hoff enthalpy and heat capacity changes upon the fraction of copolymer in aggregated form. All the transitions have the same following parametric values: ΔH_{cal}=100 kJ mol^{-1}; $T_{1/2}$=320 K; n=10, van't Hoff enthalpy and heat capacity data are as follows: a – ΔH_{vH}=1000 kJ mol^{-1}; ΔC_p= –15 kJ mol^{-1} K^{-1}; b – ΔH_{vH}=500 kJ mol^{-1}; ΔC_p= –7.5 kJ mol^{-1} K^{-1} and c – ΔH_{vH}=200 kJ mol^{-1}; ΔC_p = –3 kJ mol^{-1} K^{-1}

decreases. Clearly small van't Hoff enthalpy values and large aggregation numbers indicate that aggregation in these systems is likely to be incomplete.

How does copolymer concentration affect the transition?

One test that may be used to demonstrate that the thermal process under investigation in these studies involves aggregation is to examine the impact of varying copolymer concentration upon the transition. The mass action description of the aggregation process indicates that in an adiabatic system an increase in unimer concentration results in an increase in the amount of copolymer encountered in micellar form. And since the aggregation process is endothermic the increase in copolymer concentration should result in a temperature decrease. Viewed another way, we should be able to assert that the temperature range over which micellar aggregation occurs is reduced as the copolymer concentration is increased. In Fig. 8 experimental evidence is advanced which shows that as the copolymer concentration is increased $T_{1/2}$ decreases demonstrating the validity of this conjecture. The van't Hoff enthalpy shows a similar logarithmic relationship with copolymer concentration albeit in this case the van't Hoff enthalpy increases with increasing concentration. This arises simply because of the characteristic negative heat capacity change between the initial and final states of the thermally accessible part of the aggregation process. Indeed a plot of the van't Hoff enthalpy as a function of $T_{1/2}$ Fig. 10 is linear with a slope of –26.8 kJ mol^{-1} K^{-1}. The average model derived value for ΔC_p is –15.2(±3.4) kJ mol^{-1} K^{-1}, which is in fairly reasonable agreement.

What is the impact of co-solvents and co-solutes upon the aggregation transition?

In many applications EO–PO–EO block copolymeric surfactants will be used in formulations containing water miscible co-solvents and a variety of co-solutes.

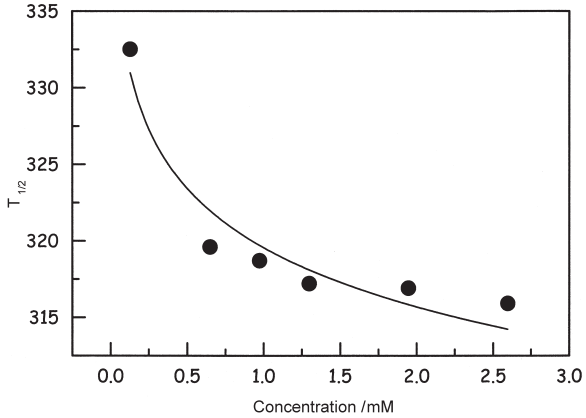

Fig. 8 The functional dependence of $T_{1/2}$ upon concentration for P237 – molecular formula $EO_{61}PO_{40}EO_{61}$

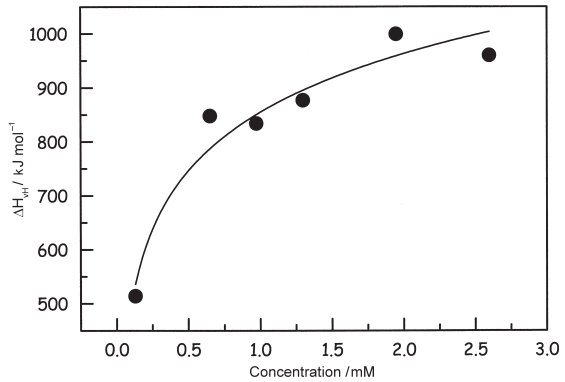

Fig. 9 The impact of changing P237 concentration upon ΔH_{vH}

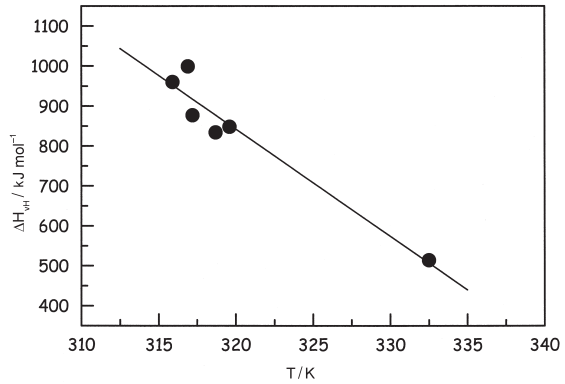

Fig. 10 A plot of ΔH_{vH} *vs.* $T_{1/2}$ for data obtained for P237. The gradient of the plot is a measure of the heat capacity change for the process

Alexandridis *et al*. [19, 20] and Armstrong *et al.* [21] have examined aspects of this in great detail.

In Fig. 11, experimental data which examines the impact of increasing methanol composition – in various methanol/water systems – upon the temperature range over which aggregation occurs, for a 5 g dm^{-3} solutions of P237 ($EO_{61}PO_{40}EO_{61}$), is shown. Clearly as the methanol composition increases the temperature range over which aggregation transition occurs also increases. In this work [21] a wide range of co-solvents and co-solutes including methanol, ethanol, propanol, butanol, urea formamide and hydrazine were used. All solutions were made up with varying ratios of water and co-additive. P237 was used as the copolymer and its concentration was kept at 5 g dm^{-3}. All the additives affected the temperature range over which aggregation occurs. The data obtained showed that the addition of fairly large quantities of co-solvents/co-solutes is required before changes in thermodynamic parameters become apparent. The effects of the co-solvents/co-solutes may be rationalised by either invoking the concept of water structure changes or by postulating some direct in-

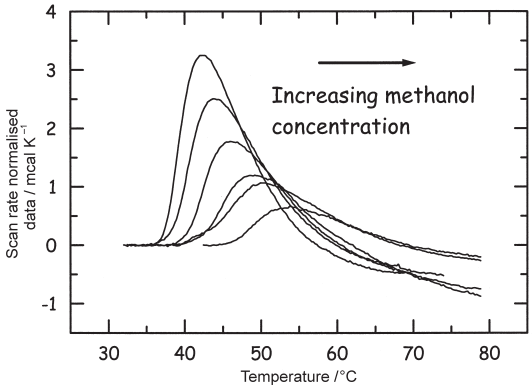

Fig. 11 Data showing the impact of increasing methanol concentration upon the aggregation transition obtained for aqueous methanol solutions of P237. Solution concentration was maintained at 5 g dm^{-3}

teraction. Methanol, ethanol, formamide and urea have been shown to raise values of the CMT (critical micelle temperature – the temperature at which micellisation commences). This may occur either because they behave as water structure breakers or because they replace water molecules in the solvation sphere of propylene oxide block – and thereby slightly stabilise the hydrated polar form of the block. Propanol, butanol and hydrazine reduce CMT values. This may occur because they either behave as water structure promoters or because they co-micellize with the polymeric surfactant [21].

$T_{1/2}$ is a particularly important parameter characterising the stability of the system. Since it is, by definition, the temperature of half completion of the aggregation process it is associated with a definite free energy. Using Eq. 4 this can be shown to be:

$$\Delta G^{\circ} = RT_{1/2} \ln(0.5^{n-1} c^{n-1} n) \tag{8}$$

For a constant value for c and n, ΔG is solely dependent upon $T_{1/2}$. Aggregation arises from a reversal of the process of hydrophobic hydration [15]. Thus $T_{1/2}$ can be linked to the stability of the solvation sphere. Changes in the stability of the solvation sphere brought about by the incorporation of a co-solvent/co-solute can thus be demonstrated by changes in $T_{1/2}$. Under these circumstances changes in ΔH_{vH} and ΔH_{cal} may be linked to the changes in $T_{1/2}$ and reflect the fact that the aggregation process is accompanied by a permanent change in heat capacity, ΔC_p. If this is the case then plots of ΔH_{vH} or ΔH_{cal} *vs*. $T_{1/2}$ should produce straight lines. All the data obtained for both ΔH_{vH} and ΔH_{cal} has been plotted with the corresponding $T_{1/2}$ values and is shown in Fig. 12. The figures obtained show a moderate amount of scatter but do suggest a reasonably linear relationship between the enthalpies and $T_{1/2}$ values. R^2 for the ΔH_{vH} *vs.* $T_{1/2}$ plot is 75% whilst for the Δ_{cal} *vs.* $T_{1/2}$ plot it is 58%. $\Delta C_{p,vH}$ the heat capacity change obtained from the ΔH_{vH} *vs.* $T_{1/2}$ plot is –12.6 kJ mol^{-1} K^{-1}. $\Delta C_{p,cal}$ the heat capacity change obtained from the Δ_{cal} *vs.* $T_{1/2}$ plot is –4.75 kJ mol^{-1} K^{-1}. Model fitting of P237 data provides the following corresponding average ΔC_p values of –15.2 kJ and –4.9 kJ mol^{-1} K^{-1} respectively. Changes in heat capacity are indicative of changes

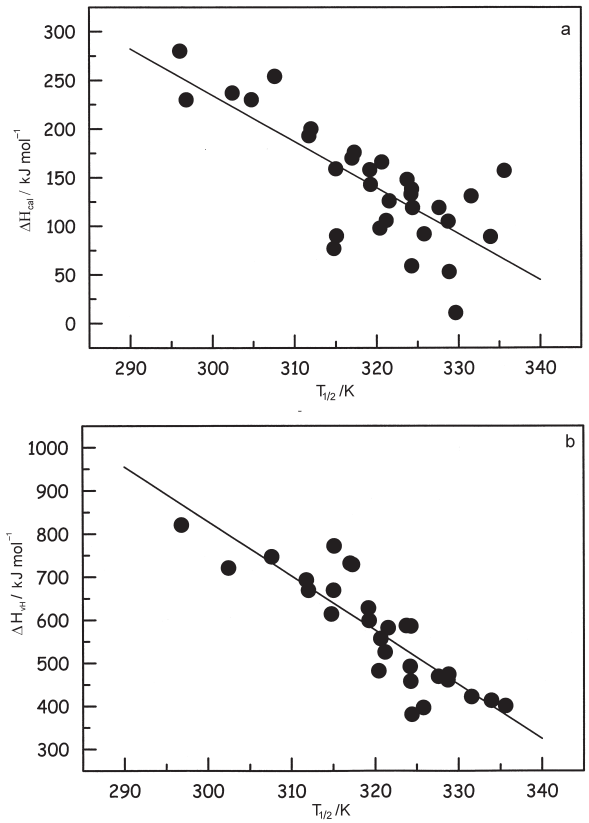

Fig. 12 a – ΔH_{cal} and b – ΔH_{vH} *vs.* $T_{1/2}$ for all the co-solvent and co-solute systems examined. P237 concentration was kept at 5 g dm^{-3}

in structure which is related to changes in cohesion [16]. It is therefore concluded that changes in $T_{1/2}$ occur because the co-solvents/co-solutes produce cohesional changes. The shift of the transition to different temperatures and the permanent change in heat capacity results in changes in ΔH_{vH} and ΔH_{cal} in agreement with Kirchoff's law [17].

Simulation of DSC signals for water/co-solvent/poloxamer systems

It is possible to obtain some indication of the size of the interaction between the co-solutes and co-solvents and the copolymer by simulation of the HSDSC output. This can be achieved in the following way [21]. Methanol and ethanol may be considered to be ligands which replace water in the solvation sphere [18] and thus bind to the copolymer molecule. This process may be represented by the following mass action expression:

$$K_L = \frac{[XL]}{[X][L]} \tag{9}$$

K_L is the ligand binding constant, [*XL*] is the concentration of polymer ligand 'complex' [*X*] is the concentration of polymer and [*L*] is the concentration of ligand. For the simulation a number of assumptions have been made. Firstly it is assumed that K_L is independent of temperature. This implies that the enthalpy of binding is either very small or indeed zero and that as a consequence K_L varies marginally, if at all, over the temperature range of interest. Secondly it is assumed that methanol, as a non-micelle-penetrating solvent [22], is desorbed from the solvation sphere prior to micelle formation. Finally, it is assumed that only one methanol molecule is linked to each oxypropylene molecular core. The justification for this comes from the observation that two water molecules are bound to each oxyethylene unit [23]. It is assumed that this must also be the maximum number of water molecules that can bind to oxypropylene units. The oxypropylene core for P237 is 40 units long which implies that at most some 80 water molecules are linked to the core. For a 1 molar methanol solution the molecular ratio of water to methanol is 55 to 1. Thus if the solvation sphere has the same composition as the bulk then each oxypropylene block should contain approximately 1 methanol molecule.

The aggregation equilibrium constant is dependent upon temperature. It is has been further noted that the enthalpy of the process is itself temperature dependent. The change in equilibrium constant with temperature should therefore be written as [24]:

$$K(T) = \frac{\exp\left[\frac{\Delta H_{vH}}{R}\left(\frac{1}{T_{1/2}} - \frac{1}{T}\right) + \frac{\Delta C_{p,vH}}{R}\left(\ln\left(\frac{T}{T_{1/2}}\right) + \frac{T_{1/2}}{T} - 1\right)\right]}{0.5^{n-1} c^{n-1} n} \tag{10}$$

where $\Delta C_{p,vH}$ is the value for the heat capacity obtained from the graph of ΔH_{vH} *vs*. $T_{½}$.

The following mass balance expressions can be drawn up for C_{Total} and L_{Total} the total concentrations of copolymer and ligand respectively:

$$\begin{aligned} C_{Total} &= [X] + [XL] + n[X_n] \\ L_{Total} &= [XL] + [L] \end{aligned} \tag{11}$$

The other symbols retain the previous definitions. Combining these expressions with the mass action expressions for aggregation and ligand binding gives:

$$nK[X]^{n+1} + nKK_L[X]^n + (L_{Total} + K_L - c)[X] - K_L c = 0 \tag{12}$$

Solving for [*X*] allows values to be obtained for [*L*] and [*XL*]. From these values the extent of aggregation, α, can be calculated:

$$\alpha = \frac{c - ([X] + [XL])}{c} \tag{13}$$

Finally it can be shown that $C_{p,xs}$ can be obtained from the following expression:

$$\phi C_{p,xs} = \frac{[\Delta H_{cal} + \Delta C_{p,cal}(T - T_{1/2})][\Delta H_{vH} + \Delta C_{p,vH}(T - T_{1/2})]}{RT^2\left(\frac{1}{\alpha} + \frac{n}{1-\alpha}\right)} + \alpha\Delta C_{p,cal} \qquad (14)$$

where $\Delta C_{p,cal}$ is the heat capacity change obtained from the graph of ΔH_{cal} *vs.* $T_{½}$ and $\Delta C_{p,vH}$ is the heat capacity change obtained from the graph of ΔH_{vH} *vs.* $T_{½}$. Using these equations it is possible to show how changes in the concentration of the ligand, L affects the HSDSC output. This is shown in Fig. 13. The figure was produced by using the thermodynamic data obtained for P237 in aqueous solution and combined with the analysis outlined above. The figure shows that the main features of the HSDSC data obtained are reproduced. Most importantly it is shown that relatively small changes in $T_{½}$ would appear to be due to a relatively small ligand binding constant. For the simulation a value of 2 was used. The dimensions of the simulated outputs decrease because of the functional dependence of the calorimetric enthalpy upon $T_{½}$. Comparison of Fig. 13 with Fig. 11 indicates that the dimensional alterations are not adequately modelled implying that either the value for $\Delta C_{p,cal}$ is in error or that there is an important enthalpic component of methanol binding to the unimeric form of the copolymer. It is also clear that though the inclusion of a term accounting for the change in heat capacity for the process reproduces the negative trend of the post-transitional portion of the traces, it is not however adequately described by the model. Undoubtedly changes in aggregation number [25], changes from spherical to rod-like micelles [26, 27] and any changes in solvation of the oxyethylene blocks are all likely to make their own separate contributions to the post-transitional heat capacity of the system.

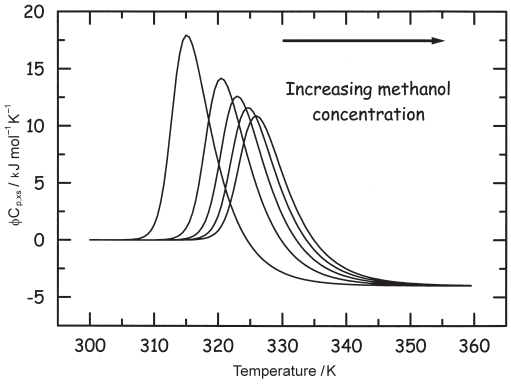

Fig. 13 Simulation of the impact of methanol upon aggregation in aqueous methanol solutions of P237

Salt effects upon aggregation

The impact of sodium chloride upon the apparent excess heat capacity/temperature function for 5 g dm^{-3} solutions of P237 and P235 ($EO_{27}PO_{39}EO_{27}$) are shown Fig. 14.

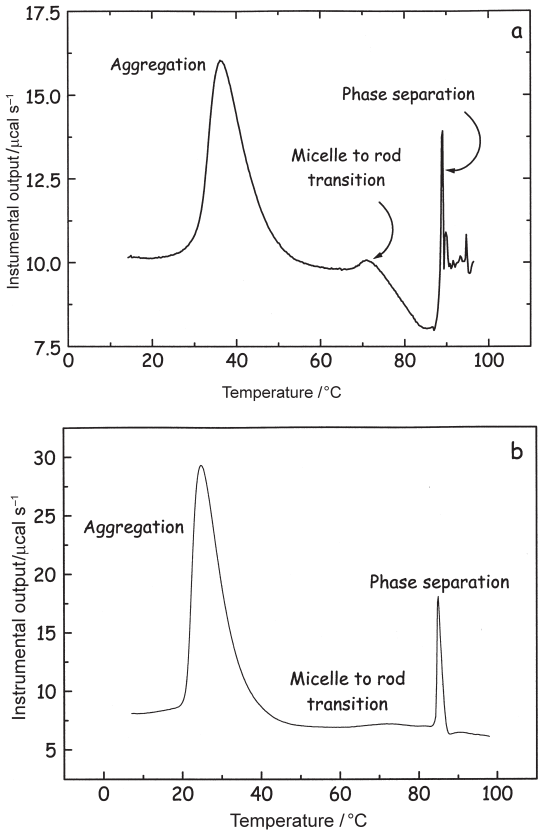

Fig. 14 Thermal signals obtained for a – P235 ($EO_{27}PO_{39}EO_{27}$) and b – P237 ($EO_{61}PO_{40}EO_{61}$) in salt solution

Comparisons between this data and previously published phase diagrams [33] permits the identification of the thermal transitions that are clearly displayed – particularly for P235.

The sphere to rod transition for P235 is characterised by a small calorimetric enthalpy (19 kJ mol^{-1}) yet the transition breadth is quite narrow – indicative of a high van't Hoff enthalpy [28]. The ratio of the van't Hoff enthalpy to the calorimetric enthalpy provides an estimate of the size of the co-operative unit [29]. In this particular instance the co-operative unit is likely to be large which might be anticipated given that the transition involves a change in shape of the micelles. Indeed it is seems quite plausible that the co-operative unit is in fact the micelle. The calorimetry literature contains extensive reports of lipid vesicle thermal transitions in which the basic co-operative unit is the vesicle itself. Estimates of the van't Hoff enthalpy were obtained in the following way. A baseline was delineated for the peak and subsequently subtracted using the software package Origin (obtained from Microcal Inc. MA). Subsequent attempts to fit the resultant data to a non-two state transition were of lim-

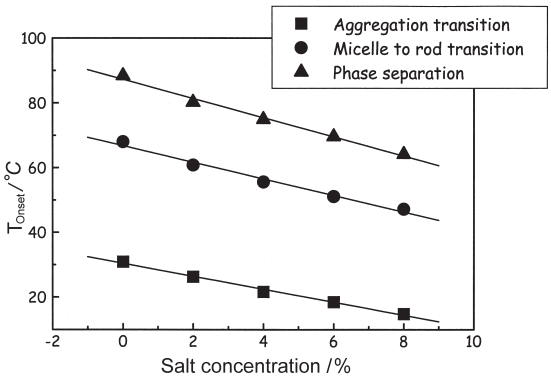

Fig. 15 The effect of increasing salt concentration upon the temperature at which aggregation, the sphere to rod transition and phase separation begin to occur in aqueous salt solutions of P235. P235 concentration was maintained at 5 g dm^{-3}

ited success. In fact it was found that the resultant data could be more appropriately fitted to a mass action description of aggregation, as outlined above. The data obtained suggested that the co-operative unit consisted of some 100 molecules and that the transition involved the aggregation of 2 to 3 units. It has been estimated that the aggregation number at 20°C is approximately 37 rising to 78 at 40°C. [30] An aggregation number of 100 at 68°C therefore seems consistent with these values. It must however be emphasised that this analysis is only tentative. No mechanistic details concerning the transition appear to have been offered in the literature. It should also be noted that if the spherical micelles are transformed into cylinders by the gradual addition of unimers – for instance by the transfer of unimers from one micelle to another – it is unlikely that this would provide the signal observed. Indeed since the unimers should already be dehydrated, there should be no net enthalpic component to the transfer. The driving force for any such transfer process would presumably originate from differences in the Laplace pressures between micelles.

Mortensen and Pedersen [30] have proposed that the changes in micellar structure are due to the huge degree of stretching of the PPO block in the micelle which is entropically unfavourable. However they also suggest that changes may occur as a result of modifications in the hydration level of the PEO blocks. This would certainly account for the marked decrease in the heat capacity accompanying the sphere to rod transition. Moreover such changes in hydration may have to be a necessary prelude to reducing the repulsion between the micelles that arises from the steric stabilisation associated the PEO blocks [31] so that the rods may be produced in the rather abrupt way demonstrated by the signal. Finally it should be noted that the sphere to rod transition in P237 is broader than that observed for P235 indicating a smaller van't Hoff enthalpy and thus presumably reflecting lower micellar aggregation numbers [32].

High sensitivity calorimetric detection and determination of the cloud point has been reported before for a number of polymers [34]. Though our work is one of the first reports where HSDSC has been used to following demixing in poloxamer solutions. This stems in part from the fact that for many of the hydrophilic poloxamers –

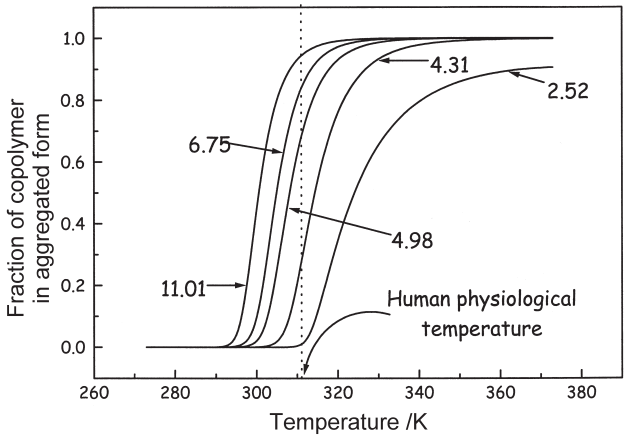

Fig. 16 Fraction of poloxamine T701, $(OE_4O_{13})_2NCH_2CH_2N(OP_{13}OE_4)_2$, in aggregated form as a function of temperature at various pH values. The vertical solid line indicates human body temperature. Concentration of T701 was 5 g dm^{-3}

such as P237 – phase separation occurs at temperatures above 100°C, the upper operating temperature of the MC2. The addition of salt presents a facile method of reducing the cloud point to temperatures into the operating range of the instrument (Fig. 15). The previously reported signals [34] are of a similar shape and size to the ones obtained in this study. The cloud point transitions for P235, however, display some additional complexity on the high temperature side of the transition which may actually arise from the instrumental response to the highly co-operative event. The authors have taken the first sharp transition in these cases to be the cloud point transition and measured the area of this peak only in order to obtain an estimate of the calorimetric enthalpy. Interestingly the cloud point peak obtained for P237 is more regular. Both transitions demonstrate that phase separation is – like the sphere to rod transition – a highly co-operative event. The calorimetric enthalpy values for P237 are in the range of 19 to 23 kJ mol^{-1} and for P235 these range from 9 to 22 kJ mol^{-1}. Estimates have been made of the van't Hoff enthalpies for P237 – again by fitting the signals to an aggregation model. These estimates have ranged from 6.7 to 9.9 MJ mol^{-1} suggesting that the co-operative unit comprises between 300 to 500 molecules and point to very big aggregate structures prior to phase separation.

Assessing the extent of micelle formation

As previously pointed out it is possible using the mass action based model outlined earlier in the text to compute the extent of micellar aggregation as a function of temperature. One use of this procedure lies in interpolating the data to show how changes in solution composition can affect the degree of micellisation under isothermal conditions. Recently we have shown how this may be done for the poloxamine block copolymeric surfactant – Tetronic 701 – molecular formula $(OE_4OP_{13})_2NCH_2CH_2N(OP_{13}OE_4)_2$ [35]. The poloxamines which are closely related to the poloxamers have a central ethylene diamine moi-

ety which renders them basic. At pH values below 10 these polymers are encountered in their protonated form. A necessary precondition for aggregation in aqueous solutions of these systems – under these conditions – is the removal of the attached proton. The extent of aggregation is therefore established by the pH of the aqueous solution. The poloxamines are used in drug delivery systems [36] it is therefore important to be able to investigate how aggregation is affected by passage through the gastrointestinal tract. For example figure. For example figure 16 shows that at human physiological body temperature and at a pH of 2.5 (approximating to stomach pH) the extent of aggregation is effectively zero; whereas at a pH of 6.8 (approximating to the pH of the duodenum) 85% of the polymer is encountered in its aggregated form. This must have some importance for the design of drug delivery systems which use poloxamines.

Conclusions

The aim of this article has been to outline how a mass action description of micellar aggregation in aqueous solutions of ethylene oxide-propylene oxide-ethylene oxide block copolymers can be used to obtain important characteristic thermodynamic data from high sensitivity DSC data obtained for the aggregation process. It has further been shown how the data can then be subsequently used to construct thermal speciation diagrams which can be used to show how aggregation is affected by changes in solution composition under isothermal conditions.

* * *

This work would not have been possible without the help of colleagues and students. In particular special mention must be made of Profs. Babur Chowdhry, Tony Beezer and John Mitchell; and Drs Jon Armstrong, Iain Paterson, Jingfeng Dong, Sham Haq and Ronan O'Brien. I would like to thank ICI and BASF for donating the copolymers. This work is supported by EPSRC grant (number GR/M 43180).

References

1 P. Alexandridis and T. A. Hatton, Colloids Surfaces A: Physicochem. Engineer. Aspects, 96 (1995) 1 and references therein.
2 R. Kjellander and E. Florin, J. Chem. Soc. Faraday Trans. I, 77 (1981) 2053.
3 J. L. Finney and A. K. Soper, Chem. Soc. Rev, 23 (1994) 1.
4 G. Karlström, J. Phys. Chem., 89 (1985) 4962.
5 W.-D. Hergeth, I. Alig, J. Lange, J. R. Lochmann, T. Scherzer and S. Wartewig, Macromol. Chem. Macromol. Symp., 52 (1991) 289.
6 M. Björling, G. Karlström and P. Linse, J. Phys. Chem., 95 (1991) 6706.
7 J. Rassing, W. McKenna, S. Bandyopadhyay and E. Eyring, J. Mol. Liq., 27 (1984) 165.
8 P. Alexandridis, V. Athanassiou, S. Fukuda and T. Hatton, Langmuir, 10 (1994) 2604.
9 B. Chu, Langmuir, 11 (1995) 414.
10 J. Armstrong, B. Chowdhry, J. Mitchell, A. Beezer and S. Leharne, J. Chem. Res. (1994) 364.
11 I. Patterson, J. Armstrong, B. Chowdhry and S. Leharne, Langmuir, 13 (1997) 2219.
12 J. Sánchez-Ruiz, J. López-Lacomba, M. Cortijo and P. Mateo, Biochem., 27 (1988) 1648.

13 S. Leharne, Chapter 25 in Biocalorimetry Eds J. Ladbury and B. Chowdhry, J. Wiley and Sons, Chichester 1998.
14 C. Tanford, The Hydrophobic Effect: Formation of Micelles and Biological Membranes, Wiley, New York 1980.
15 T. Sobisch and R. Wüstnick, Colloids Surfaces, 62 (1992) 187.
16 L. Andreoli-Ball, S. J. Sun, L. M. Trejo, M. Costas and D. Patterson, Pure and Appl. Chem., 62 (1990) 2097.
17 P. W. Atkins, Physical Chemistry, 5th Edition, Oxford University Press, Oxford 1994.
18 W. E. Waghorne, Chem. Soc. Rev., 22 (1993) 285.
19 R. Ivanova, B. Lindman and P. Alexandridis, Adv. Coll. Inter. Sci., 89–90 (2001) 351.
20 R. Ivanova, P. Alexandridis and B. Lindman, Coll. Surf. A: Physicochem. Eng. Aspects, 183–185 (2001) 41.
21 J. Armstrong, B. Chowdhry, J. Mitchell, A. Beezer and S. Leharne J. Phys. Chem., 100 (1996) 1738.
22 M. E. Emerson and A. Holtzer, J. Phys. Chem., 71 (1967) 3321.
23 P. Bloss, W.-D. Hergeth, E. Döring, K. Witkowski and S. Wartewig, Acta Polymerica, 40 (1989) 260.
24 J. F. Brandts and L.-N. Lin, Biochemistry, 29 (1990) 6927.
25 J. Rassing and D. Attwood, Int. J. Pharm., 47 (1983) 55.
26 P. Linse, Macromolecules, 26 (1993) 4437 and J. Phys. Chem., 97 (1993) 13896.
27 K. Mortensen, Europhys. Lett., 19 (1992) 599.
28 B. Chowdhry and S. Leharne, J. Chem. Ed., 1997.
29 J. Armstrong, B. Chowdhry, R. O'Brien, A. Beezer, J. Mitchell and S. Leharne, J. Phys. Chem., 99 (1995) 4590.
30 K. Mortensen and J. S. Pedersen, Macromolecules 26 (1993) 805.
31 G. Wanka, H. Hoffmann and W. Ulbricht, Colloid Polym. Sci., 268 (1990) 101.
32 K. Mortensen and W. Brown, Macromolecules, 26 (1993) 4128.
33 J. Armstrong, B. Chowdhry, M. Snowden and S. Leharne, Langmuir, 14 (1998) 2004.
34 H. G. Schild and D. A. Tirrell, J. Phys. Chem., 94 (1990) 4352.
35 J. Armstrong, B. Chowdhry, M. Snowden, J. Dong and S. Leharne, Int. J. Pharm., (in press).
36 S. M. Moghimi and A. Hunter, C. Tibtech, 18 (2000) 412.
37 E. Hecht and H. Hoffmann, Coll. Surf. A: Physicochem. Eng. Aspects, 96 (1995) 181.
38 B. Z. Chowdhry, M. J. Snowden and S. A. Leharne, J. Phys. Chem., 101 (1997) 10226.